

REE characteristics of the Fanshan alunite deposit in Zhejiang Province, China*

HE Yuliang (何玉良)^{1,2}, ZHANG Qian (张乾)^{1**}, SHAO Shuxun (邵树勋)¹, ZHU Xiaoqing (朱笑青)¹, ZHU Chaohui (祝朝辉)^{1,2}, and WANG Dapeng (王大鹏)^{1,2}

¹ Key Laboratory of Ore Deposit Geochemistry, Institute of Geochemistry, Chinese Academy of Sciences, Guiyang 550002, China

² Graduate School, Chinese Academy of Sciences, Beijing 100039, China

Abstract REE geochemistry data from the Fanshan alunite deposit indicated that its ore-forming materials came chiefly from the country rocks, with $\delta\text{Ce} > 0$ for alunite ores. According to the differences in δEu , the alunite ores were divided into three types: weak negative Eu anomaly, weak positive Eu anomaly and remarkable positive Eu anomaly. The phenomena of Ce-enrichment in the ores indicated that the Fanshan alunite deposit was formed in an oxidizing environment. Variations in f_{O_2} are corresponding to those in δEu : Eu anomaly varies from negative to positive with increasing f_{O_2} . And two other important factors may impact the occurrence of Eu anomalies: the contents of alkaline feldspar and the protolith structure in the mineralization period.

Key words REE characteristics; volcanism; alunite deposit; Fanshan, Zhejiang

1 Introduction

Alunite $[\text{KAl}_3(\text{SO}_4)_2(\text{OH})_6]$ is a very important non-ferrous metal resource, so many countries throughout the world have made great investments in research on the mechanism of its formation, its geological characteristics and applications. Overseas scientists have made deep-going studies on the geochemical characteristics of alunite deposits, including the physical and chemical conditions of alunite mineralization (Hemly et al., 1969), stable isotopes, REE distribution patterns, mineralization ages (Cunningham et al., 2004; Mutlu et al., 2005) and Na-K exchange between alunite and aqueous sulfate solutions (Stoffregen and Cygan, 1990). The Fanshan alunite deposit is one of the super-large alunite deposits in the world, with a glorious mining history. Early in the 1930s of the last century, Ye Liangfu

(1931) had made research on this deposit and pointed out that this deposit was of post-magmatic hydrothermal origin. And after that, there were proposed some different hypotheses concerning the origin of the deposit, e.g. low temperature hydrothermal hypothesis^①, volcano-hydrothermal hypothesis^②, volcano-sedimentation-hydrothermal reworking hypothesis^③ (Tang Yuanlong, 1992), etc. Wang Fusheng et al. (1997) indicated the Fanshan alunite deposit had resulted from repeated metasomatism-alteration between acid volcanic hydrothermal solutions and pyroclastic rocks, and Liang Xiangji and Wang Fusheng (1998) came into the same conclusion through simulating experiments. Little geochemical research had been done. Up to now, major element analyses (Wang Fusheng et al., 1997), REE analyses (Xuan Ziqiang, 1998; Zhou Xinhua et al., 1998; Ren Shengli and Zhou Xinhua, 1997) and isotopic ages (Ren Shengli et al., 1998) are less available. Many studies indicated that the REEs play a very important role in constraining the mineralizing environment and ore genesis of the deposit (Bi Xianwu and Hu Ruizhong, 1998; Yang Yaoming et al., 2004; Guan Tao et al., 2005). This paper presents the REE characteristics of the Fanshan alunite deposit and their geological implications.

2 Geological characteristics of the Fanshan alunite deposit

The Fanshan alunite deposit is the biggest alunite deposit so far discovered in our country, which is

ISSN 1000-9426

* This research project was financially supported jointly by the Key Research Project (No. KZCX3-SW-125) of CAS and the National Natural Science Foundation of China (No. 40172037).

** Corresponding author, zhqiangel@163.com.

① Sun Yue (1964) Geological exploration report of the Fanshan alunite deposit in Zhejiang Province, China.

② Cheng Yilang (1984) Geological exploration report of the Fanshan alunite deposit in Zhejiang Province, China.

③ Lin Qi (1980) The metallogenic regularity and ore-seeking direction of alunite deposits in Zhejiang Province, China.

located at the boundary of Cangnan County and Wenzhou City, Zhejiang Province. Geotectonically, it is located in the eastern part of the Hercynian-Indosinian fold belt along the coastal area of Southeast Zhejiang, in the southeast tectonic zone of the Chinese tectonic plate. In the mining area intermediate-acid pyroclastic rocks and volcanic tuffs are widespread, in addition to some rhyolites. The major intrusive rocks in the area are rhyolite porphyry and diabase. Appearing in the area studied are the strata varying from old to young, which may be divided into 3 formations: (1) the Upper Jurassic Gaowu Formation (J_{3g}): this formation consists of caesious dense massive lithic-crystal flood tuff; (2) the Lower Cretaceous Chaochuan Formation (K_{1c}): this formation consists of intermediate-acid pyroclastic rocks, volcanic lavas and some sedimentary tuffs, and it is the main metallogenic belt. The alunite orebody lies in the second submember of the first member of this formation (K_{1c}^{1-2}); and (3) the Quaternary (Q): alluvial drift bed (Fig. 1).

The alunite deposit is located in the Fanshan broken crater. Faulted structure was developed very well, and there were recognized a total of 52 faults of different sizes. All the faults were classified as 2 groups: ring faults and radial faults. The alunite

orebody is of arc-sharp distribution along the circular structure of the Fanshan broken crater. Rocks cconnected with metallogenesis are comprised mainly of brecciform tuff, detratus-crystal tuff and vitric tuff. Because of the different characteristics of these three country rocks, the degree of mineralization also showed significant differences (Table 1). Important wall-rock alterations include silicification, alunization, pyrophyllitic alteration, sericitization, kaolinitization and pyritization.

The orebodies have a total length of about 10 km, developed from the north to the south are the Pingpengling, Dagangshan, Shuiweishan, Jilongshan, and Mabishan, respectively. Especially the Shuiweishan orebody located in the center of the mining area is the best one not only in grade, but also in ore quality. The ore deposit shows a precise stratification, altogether 6 ore beds can be divided. These ore beds constutite 2 ore belts: the upper ore belt (ore bodies Nos. 1, 2 and 3) is the main ore bed of the Fanshan alunite deposit.

Alunite ores are grayish-white and gray in color, and high-grade ores show an oily luster. According to their sizes, the alunite ores were divided into three kinds: brecciform ore, coarse-grained ore and dense dacitic ore. The alunite mineral is cryptocrystalline, so

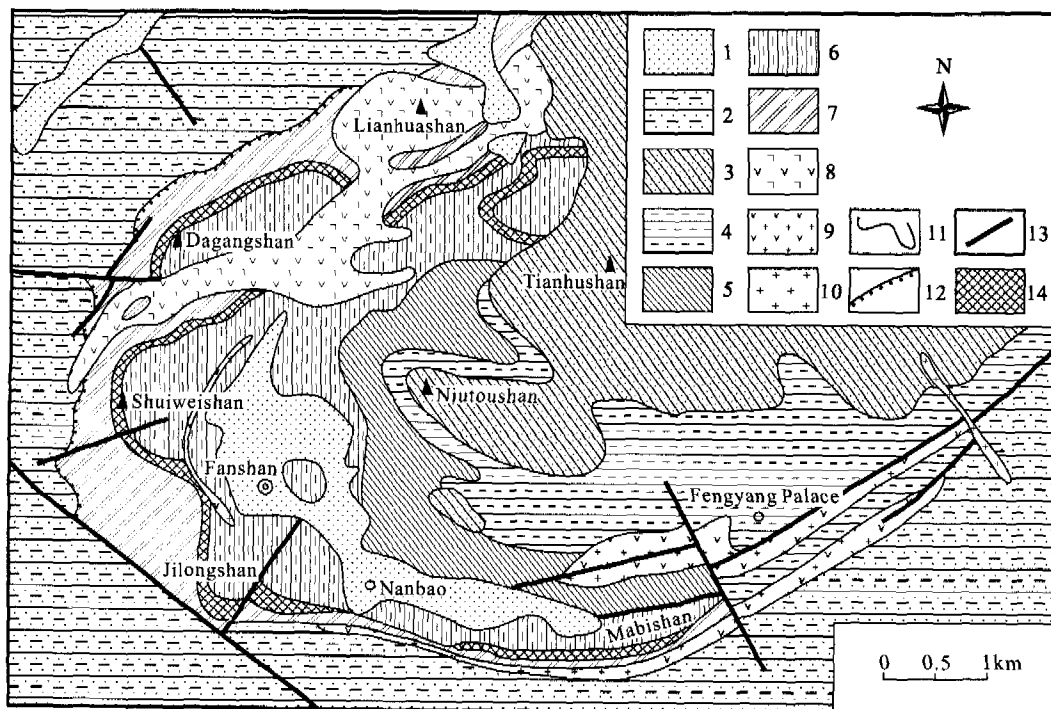


Fig. 1. The geological sketch map of the Fanshan alunite deposit in Zhejiang Province (after Wang Fusheng et al., 1997). 1. Q^{3-4} Quaternary alluvial drift bed; 2. J_{3g} dacitic lithic-crystal welded tuff; 3. K_{1c}^{2-2} rhyolite, rhyolitic breccia tuff, rhyolite porphyry, rhyolitic vitric flood tuff; 4. K_{1c}^{2-1} andesite and andesitic crystal-lithic breccia tuff; 5. K_{1c}^{1-4} filemot, grayish-white and purplish-gray pelitic siltstone, tuffaceous siltstone, siltstone, conglomerate and tuff; 6. K_{1c}^{1-3} purplish-gray tuffaceous gravel sandstone, siltstone and silty mudstone; 7. K_{1c}^{1-2} purple siltstone, gravel sandstone, conglomerate, filemot microsandstone and tuffaceous gravel sandstone; 8. $\nu\pi$ felsophyre; 9. λ rhyolitic vein; 10. $\lambda\pi$ rhyolite porphyry; 11. geological boundary; 12. unconformable interface; 13. fault; 14. orebody.

Table 1. Characteristics of the ore-host rocks and mineralization of the Fanshan alunite deposit

Rock type	Characteristics and mineral composition	Characteristics of mineralization
Brecciform tuff	Composed mainly of lapilli and pyroclast	Porosity is big, easily to form breccia ore—low-grade ore
Detritus-crystal tuff	Composed of pyroclastics and volcanic crystals; major minerals in the crystals are quartz, feldspar and biotite	Porosity is medium, easily to form ore; degree of mineralization is high
Vitric tuff	Composed of glass debris and volcanic ash; minerals in the crystals are alkaline feldspar and quartz	Porosity is small, hard to form ore; the degree of mineralization is low

it is difficult to distinguish. Electron microprobe analysis indicated that matrix mineral was alunite while the big crystal was quartz, and the opaque mineral was magnetite. The main component of the ore was K-alunite, especially in high-grade ores the contents of K-alunite could reach 80%. Other mineral components were Na-alunite, quartz, hematite, pyrophyllite, sericite and kaolinite. Quartz, mica and fluorite veins were occasionally found filling in the crevasses of the ores. But pyrite was hard to find.

The mineralization age of the deposit is 73–95 Ma (Zhou Xinhua et al., 1998; Ren Shengli et al., 1998), while the age of the regional strata is 87–110 Ma (Hu Huaguang et al., 1984), and the K-Ar age of the country rocks directly connected with the alunite deposit is 95–101 Ma. On the contrary, the mineralization of the Fanshan alunite deposit is later than the volcanic activity by 10–20 Ma.

3 Samples and methodology

Samples used in this work were collected from the three blocks in the Fanshan alunite deposit: the Jilongshan, Dagangshan and Shuiweishan. Samples of volcanic host rock were collected from the back of the Dagangshan Mountain at an interval of 3 kilometers. Both the mineralized country rocks and ores were collected from the three ore occurrences. Gypsum was collected from the Dagangshan, which occurs among different alunite ore beds. Gypsum is a sedimentary mineral from a volcanic lake formed at the intermittent stage of volcanic eruption. All the samples in this study are whole-rock samples because the alunite mineral is cryptocrystalline.

In order to reveal the REE distribution characteristics of alunite ores, mineralized country rocks and unaltered igneous rocks, 34 samples were analyzed and 30 sets of effective data and 4 sets of invalid data were acquired. The effective data include those of 21 ores, 4 mineralized country rocks (Fsh-18, Fsh-26, Fsh-87, Fsh-96), 2 intrusive rocks (Fsh-30, Fsh-74), 1 volcanic host rock (Fsh-61), and gypsum (Fsh-99).

Sample pre-treatment was carried out at State Key Laboratory of Ore Deposit Geochemistry,

Institute of Geochemistry, Chinese Academy of Sciences (CAS). The contents of trace elements in the samples were determined by ICP-MS at the National Research Center for Geoanalysis, Chinese Academy of Geological Sciences (CAGS), Beijing. The analysis method was described by Qi Liang et al. (2000). In the analysis process, the domestic sample standard GSR-5 was adopted. The analytical precision is 5% and the analytical error is 10%. The analysis results are listed in Table 2.

4 REE characteristics of the Fanshan alunite deposit

4.1 REE characteristics of volcanic and sub-volcanic rocks

The δEu values of the country rocks are within the range of 0.72–0.97, with almost no Eu depletion; the δCe values, 0.85–1.08, with no obvious anomaly; $\sum\text{REE}=29.4\text{--}114.52$, $\sum\text{HREE}=1.60\text{--}2.15$, and $(\text{La}/\text{Yb})_{\text{N}}=21.00\text{--}117.02$. Because of LREE enrichment and HREE depletion, the REE distribution pattern belongs to a typical LREE-enrichment distribution pattern (Fig. 2). And there occurred obvious LREE fractionation, with $(\text{La}/\text{Sm})_{\text{N}}$ values varying from 14.76–26.37; but there occurred not so remarkable HREE fractionation as the LREE fractionation, with $(\text{Gd}/\text{Yb})_{\text{N}}$ values varying between 0.86 and 1.78. Xie

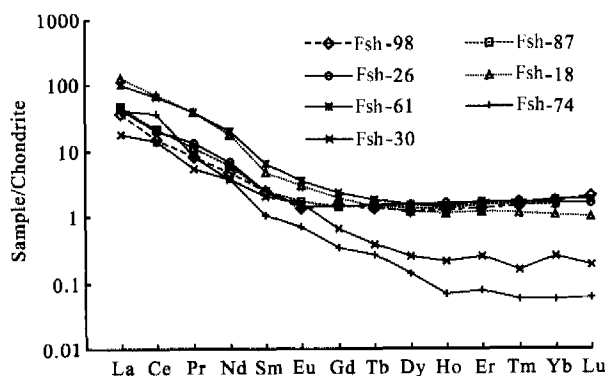


Fig. 2. Chondrite-normalized REE distribution patterns of volcanic and sub-volcanic rocks from the Fanshan alunite deposit (chondrite REE data from Boynton, 1984).

Jiaying and Tao Kuiyuan (1996) found that the chondrite-normalized REE distribution patterns in southeastern Zhejiang are characterized by LREE enrichments in her study of different igneous cycles of the Mesozoic era. And the slope of LREE patterns is

bigger than that of the HREE patterns, and medium-high negative Eu anomalies are recognized. These results are consistent with the findings by Zhou Xinhua et al. (1998), Yang Xiaochun (1998) and Gu Mingguang (2003). In a word, the REE distribution

Table 2. REE composition of the Fanshan alunite deposit ($\times 10^{-6}$) and REE parameters

Ore type Sample No.	Massive ore													Mega-grained ore
	fsh-7	fsh-17	fsh-25	fsh-42	fsh-44	fsh-48	fsh-71	fsh-78	fsh-79	fsh-83	fsh-103	fsh-104	fsh-105	fsh-49
La	70.30	26.50	50.00	28.20	21.60	53.20	17.40	2.12	23.60	37.30	11.20	6.34	15.50	79.00
Ce	137.00	42.80	60.50	34.50	26.20	71.40	34.00	21.50	34.60	41.70	18.60	21.20	39.00	99.70
Pr	15.00	3.10	5.12	2.23	1.66	5.22	1.29	0.23	1.68	3.35	1.49	0.76	2.17	7.35
Nd	55.40	6.12	14.30	4.59	3.25	10.60	2.63	0.57	3.61	8.68	3.71	2.05	5.74	16.00
Sm	9.45	0.37	2.43	0.55	0.34	0.82	0.25	0.06	0.43	0.95	0.38	0.22	0.57	1.12
Eu	2.05	0.15	0.64	0.18	0.13	0.22	0.09	0.03	0.15	0.20	0.12	0.08	0.13	0.24
Gd	6.82	0.22	2.23	0.42	0.19	0.59	0.21	0.06	0.36	0.51	0.22	0.12	0.26	0.47
Tb	0.92	0.05	0.29	0.07	0.04	0.08	0.03	0.01	0.07	0.07	0.05	0.02	0.04	0.10
Dy	6.35	0.34	1.13	0.35	0.27	0.32	0.19	0.04	0.37	0.48	0.36	0.10	0.22	0.44
Ho	1.41	0.08	0.17	0.08	0.07	0.06	0.05	0.01	0.07	0.10	0.08	0.03	0.05	0.07
Er	3.44	0.27	0.49	0.25	0.22	0.17	0.18	0.03	0.21	0.33	0.25	0.11	0.16	0.24
Tm	0.53	0.04	0.06	0.04	0.04	0.02	0.03	0.00	0.03	0.05	0.04	0.02	0.03	0.03
Yb	2.73	0.28	0.44	0.28	0.25	0.15	0.19	0.03	0.21	0.33	0.28	0.15	0.22	0.24
Lu	0.42	0.04	0.06	0.04	0.04	0.02	0.02	0.00	0.03	0.05	0.04	0.03	0.03	0.04
Σ REE	311.85	80.37	137.87	71.80	54.30	142.86	56.56	24.67	65.42	94.10	36.82	31.20	64.11	205.03
Σ LREE	289.21	79.00	132.99	70.30	53.18	141.45	55.66	24.51	64.07	92.18	35.49	30.64	63.11	203.41
Σ HREE	22.64	1.32	4.87	1.52	1.12	1.41	0.90	0.17	1.35	1.92	1.32	0.56	1.01	1.62
(La/Yb) _N	17.34	64.00	77.14	67.90	57.30	234.43	62.73	52.94	76.50	75.52	26.59	29.29	48.16	222.85
(La/Sm) _N	4.68	44.57	12.92	32.25	40.20	41.01	43.61	23.81	34.85	24.59	18.74	18.47	17.08	44.33
(Gd/Yb) _N	2.01	0.64	4.12	1.21	0.60	3.11	0.91	1.79	1.40	1.24	0.63	0.66	0.97	1.59
δ Eu	0.78	1.58	0.84	1.15	1.56	0.95	1.13	1.58	1.16	0.86	1.32	1.46	1.00	0.99
δ Ce	1.02	1.14	0.91	1.05	1.05	1.03	1.73	7.41	1.32	0.90	1.10	2.33	1.62	1.00

Ore type Sample No.	Mega-grained ore			Pebble ore				Gypsum	Mineralization rock			Host rock	Rhyolite	Beschtaiuite
	fsh-80	fsh-51	fsh-99	fsh-34	fsh-54	fsh-76	fsh-88	fsh-99	fsh-18	fsh-26	fsh-98	fsh-61	fsh-30	fsh-74
La	5.18	5.92	9.31	2.37	2.78	9.10	9.63	11.40	39.40	13.40	11.40	31.30	5.61	13.20
Ce	22.60	22.90	16.00	10.50	16.20	14.40	14.40	20.40	56.80	16.00	11.80	55.00	11.20	29.70
Pr	0.29	0.55	0.99	0.24	0.28	0.90	0.86	2.23	4.66	1.60	0.98	4.80	0.66	0.98
Nd	0.60	1.27	2.31	0.56	0.65	2.71	2.15	7.32	10.90	4.07	2.92	12.20	2.28	2.27
Sm	0.05	0.13	0.43	0.04	0.04	0.57	0.28	1.15	0.94	0.48	0.49	1.23	0.40	0.21
Eu	0.03	0.04	0.18	0.03	0.04	0.11	0.10	0.17	0.22	0.11	0.10	0.27	0.12	0.05
Gd	—	0.08	0.53	—	0.12	0.20	0.26	0.71	0.50	0.38	0.39	0.60	0.17	0.09
Tb	0.01	0.01	0.05	0.01	0.01	0.02	0.04	0.11	0.07	0.07	0.06	0.09	0.02	0.01
Dy	0.03	0.06	0.19	0.06	0.06	0.09	0.30	0.92	0.39	0.51	0.39	0.49	0.08	0.05
Ho	0.01	0.01	0.03	0.01	0.01	0.01	0.07	0.29	0.08	0.12	0.09	0.10	0.02	0.01
Er	0.03	0.04	0.10	0.06	0.05	0.06	0.26	1.00	0.26	0.35	0.29	0.36	0.05	0.02
Tm	0.00	0.00	0.02	0.01	0.01	0.01	0.05	0.17	0.04	0.06	0.05	0.05	0.01	0.00
Yb	0.03	0.04	0.16	0.07	0.05	0.06	0.29	1.03	0.23	0.35	0.37	0.39	0.05	0.01
Lu	0.00	0.00	0.03	0.01	0.01	0.01	0.05	0.17	0.03	0.05	0.07	0.06	0.01	0.00
Σ REE	28.87	31.05	30.32	13.96	20.29	28.23	28.75	47.02	114.52	37.54	29.40	106.95	20.67	46.59
Σ LREE	28.76	30.80	29.21	13.74	19.98	27.77	27.43	42.62	112.92	35.66	27.69	104.80	20.27	46.40
Σ HREE	0.11	0.25	1.11	0.22	0.31	0.45	1.32	4.40	1.60	1.89	1.71	2.15	0.40	0.18
(La/Yb) _N	105.83	102.29	40.24	23.45	38.21	102.13	22.17	7.45	117.02	25.81	21.00	53.70	70.05	741.61
(La/Sm) _N	62.66	29.31	13.68	33.81	43.67	10.10	21.49	6.25	26.37	17.42	14.76	15.98	8.82	39.92
(Gd/Yb) _N		1.66	2.74		1.93	2.69	0.72	0.56	1.78	0.88	0.86	1.23	2.54	6.05
δ Eu		1.18	1.13		1.74	1.02	1.15	0.57	0.97	0.77	0.72	0.95	1.38	1.18
δ Ce	4.42	3.07	1.27	3.35	4.43	1.21	1.20	0.97	1.01	0.83	0.85	1.08	1.40	1.99

patterns of volcanic rocks in the mining area are similar to those of the Mesozoic volcanic rocks except that their negative Eu anomalies are less remarkable than those found in other areas.

For rhyolite, $\sum\text{REE}=20.67$, $\delta\text{Eu}=1.38$ and $\delta\text{Ce}=1.40$, with positive Eu and Ce anomalies. The $(\text{La}/\text{Sm})_N$ value is 8.82 and the $(\text{Gd}/\text{Yb})_N$ value is 2.54. The $\sum\text{REE}$ value of sub-volcanic rocks is 46.59, and $(\text{La}/\text{Sm})_N=39.91$, $(\text{Gd}/\text{Yb})_N=6.05$, $\delta\text{Eu}=1.18$, $\delta\text{Ce}=1.99$, also with positive Eu and Ce anomalies.

4.2 REE characteristics of alunite ores

The REE characteristics of alunite ores are very complicated. Accordingly, the alunite ores can be classified as three types: I. weak positive Eu anomaly; II. remarkable positive Eu anomaly; and III. weak negative Eu anomaly.

4.2.1 Weak positive Eu anomaly

Both ores of this type show weak positive Eu and Ce anomalies, with $\delta\text{Eu}=1.00-1.58$ and $\delta\text{Ce}=1.05-1.62$. As compared with the country rocks, no significant difference is noticed. As viewed from $\sum\text{REE}=27.43-74.04$, $\sum\text{LREE}=28.23-79.04$, $\sum\text{HREE}=0.45-1.52$ and $(\text{La}/\text{Yb})_N=22.1-102.13$, the ores belong to the LREE-enrichment type and they are characterized by $(\text{La}/\text{Sm})_N=10.10-44.57$, $(\text{Gd}/\text{Yb})_N=0.64-2.74$, strong LREE fractionation and smooth HREE pattern. The REE distribution patterns (Fig. 3a) are similar to those of igneous rocks (Fig. 2).

4.2.2 Remarkable positive Eu anomaly

Ores of this type show remarkable positive Eu and Ce anomalies, with δEu values within the range of 1.18-1.74, and δCe values, 2.33-7.41. Compared with the country rocks and type-I ores, the total REE amount is low ($\sum\text{REE}=13.96-31.20$) with strong LREE enrichment: $\sum\text{LREE}=13.74-30.60$, $\sum\text{HREE}=0.11-0.56$, and $(\text{La}/\text{Yb})_N=23.45-105.83$. At the same time, LREE fractionation is stronger than that of the type-I ores, with $(\text{La}/\text{Sm})_N=18.47-62.66$; HREE fractionation is also obvious, with $(\text{Gd}/\text{Yb})_N=0.66-1.99$. According to their REE distribution patterns, the type-II alunite ores are significantly different from igneous rocks (Fig. 3b).

4.2.3 Weak negative Eu anomaly

The REE distribution patterns of type-III alunite ores are most similar to those of the country rocks (Fig. 3c). Type-III ores are characterized by weak negative Eu anomalies, with $\delta\text{Eu}=0.78-0.99$, just like the country rocks. And the δCe values are also close to

those of the country rocks and Type-I ores, with $\delta\text{Ce}=0.90-1.03$. But the total amounts of REE, LREE and HREE are much higher than those of the volcanic rocks and other types of ores, with $\sum\text{REE}=94.10-311.85$, $\sum\text{LREE}=92.18-289.21$, and $\sum\text{HREE}=1.92-22.64$. Obvious HREE and LREE fractionations occurred, with $(\text{La}/\text{Sm})_N=4.68-44.33$ and $(\text{Gd}/\text{Yb})_N=1.24-2.01$. Type-III ores are characterized by LREE enrichment, with $(\text{La}/\text{Yb})_N=17.34-234.43$, and the extent of REE fractionation in the ores is more significant than that of the other two types of ores.

These three types of ore have some common characteristic features as described below:

(1) All the REE distribution patterns are of the LREE-enrichment type, with varying HREE depletion, especially those of the ores of type-III.

(2) There are displayed remarkable positive Ce anomalies, except for a few ores which show weak

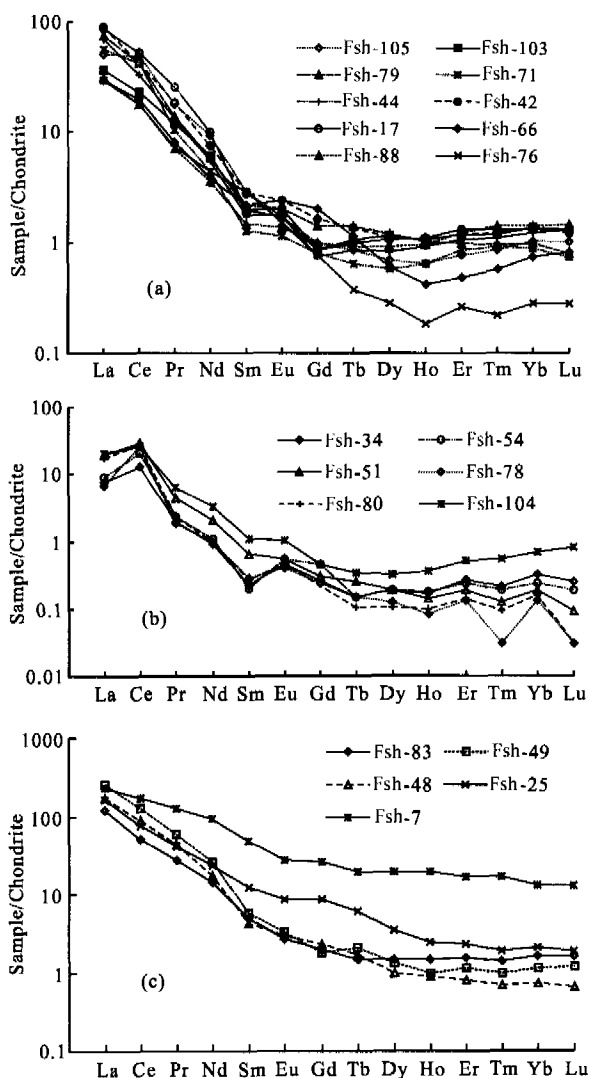


Fig. 3. Chondrite-normalized REE distribution patterns of ores from the Fanshan alunite deposit (chondrite REE data from Boynton, 1984).

negative anomalies.

(3) Compared with the country rocks, Eu is concentrated in the ores showing remarkable positive anomalies except for type-III ores.

(4) The REEs are concentrated largely in the ores, with $\sum\text{REE}$ in the ore being much higher than that in the country rocks, especially for the type-III ores.

From the REE distribution patterns of the country rocks and ores (Figs. 2 and 3), we can see that the REE distribution patterns have some common characteristics in addition to differences. Firstly, all the REE distribution patterns are right-inclined, as those in the intermediate-acid volcanic rocks, characterized by LREE enrichment and HREE depletion. Secondly, the type-III ores show weak negative anomalies, just as the country rocks. Finally, their $(\text{Sm}/\text{Nd})_N$ ratios are very close to one another, with the values of 0.06–0.21 for the ores and the values of 0.09–0.17 for the country rocks. Accordingly, it is concluded that the country rocks and alunite ores are believed to be of the same origin.

4.3 REE characteristics of gypsum

Shown in Fig. 4 are the REE distribution patterns with $\sum\text{REE}=47.02$, $\sum\text{LREE}=42.62$, $\sum\text{HREE}=4.40$ and $(\text{La}/\text{Yb})_N=7.45$, indicative of the LREE-enrichment type. Eu depletion is very obvious, $\delta\text{Eu}=0.57$; no Ce anomaly, $\delta\text{Ce}=0.97$. And $(\text{La}/\text{Sm})_N=6.25$, $(\text{Gd}/\text{Yb})_N=0.56$, in contrast to HREE, and LRRE fractionation is remarkable.

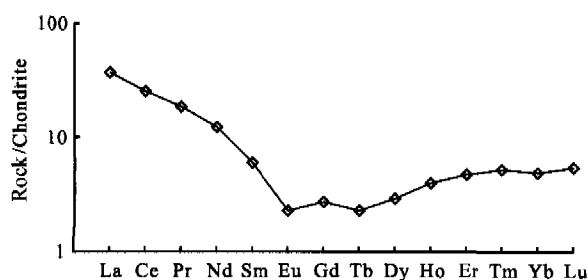


Fig. 4. Chondrite-normalized REE distribution patterns of gypsum from the Fanshan deposit (chondrite REE data from Boynton, 1984).

It is found that the REE composition of alunite is different from that of gypsum, though both of them belong to sulfate minerals. It may be indicated that they have different ore-forming mechanisms. Gypsum is the product of direct sedimentation in a volcano-sedimentary basin, while alunite resulted from the interaction between SO_4^{2-} -bearing hydrothermal solutions and igneous rocks.

5 Analysis and discussion

The Eu and Ce anomalies are attributed to the

variable valence of the two elements (Wang Zhonggang et al., 1989). In the reducing environment Eu is present as Eu^{2+} , and its ionic radius increases. Therefore, in response to the variation of its properties, it is separated from other rare-earth elements. The occurrence of Ce anomaly is due to the presence of Ce^{4+} in the oxidizing environment (Ding Zhengju et al., 2003). Because of the intensifying variation and the decrease of ionic radius, Ce^{4+} would find its way into the mineral lattice and thus would be separated from other REEs. So, the Eu and Ce anomalies can reflect a redox environment during the mineralization period.

As shown in Fig. 2 and listed in Table 2, the ores show varying Eu anomalies from weak negative to weak positive, then to positive, and display significant differences from the country rocks. There may be two factors leading to the occurrence of positive Eu anomalies:

(1) The effects of alkali feldspar. Feldspar has a big partition coefficient of Eu as compared to the other rare-earth elements, so Eu is easy to concentrate in feldspar phenocrysts, giving rise to positive Eu anomalies. For example, Klinkhammer et al. (1994) made use of the reaction between feldspar and ions in the solution to explain the Eu anomalies appearing in the REE distribution patterns of hydrothermal fluids in the mid-ocean ridges. The alunite resulted mainly from metasomatism of alkaline feldspar by ore fluid, thus making Eu highly concentrated in alunite crystals, so the alunite ores show positive Eu anomalies. Liang Xiangji et al. (1998) pointed out that the formation of alunite ore is closely related with the composition and texture of the protoliths and the quality of the alunite is determined by the contents of alkaline feldspar and the porosity of the igneous rocks. As the protoliths are different in properties, their contents of alkaline feldspar and porosity are distinct. Therefore, the alunite ores show different Eu anomalies.

(2) Variations in f_{O_2} and temperature during the mineralization period. The ore-forming system was an open acidic oxidation system whose oxygen fugacity (f_{O_2}) was high, so Eu was present mainly in the form of Eu^{3+} . Eu^{3+} replaced K^+ and Na^+ of the alunite mineral and found way into the lattice and then was concentrated in the alunite ore. Bau (1991) indicated that there existed close relations among f_{O_2} , temperature, pressure and pH when the redox system of $\text{Eu}^{2+}/\text{Eu}^{3+}$ was in equilibrium: with increasing temperature, the $\text{Eu}^{2+}/\text{Eu}^{3+}$ redox potential tended to increase drastically (i.e. the equilibrium shifted towards higher f_{O_2}); with increasing pH, the $\text{Eu}^{2+}/\text{Eu}^{3+}$ redox potential increased slightly; with increasing pressure, the $\text{Eu}^{2+}/\text{Eu}^{3+}$ redox potential decreased very slightly (Fig. 5). The ore-forming temperature of the Fanshan alunite deposit was estimated at 150–350°C,

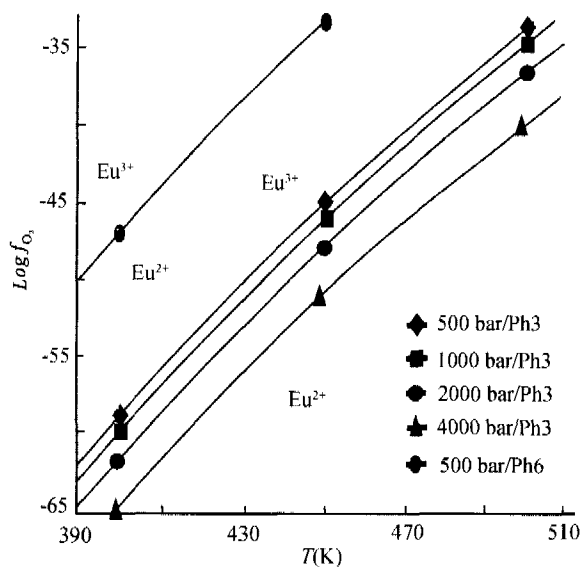


Fig. 5. The $\text{Eu}^{3+}/\text{Eu}^{2+}$ ratios in the case of redox equilibrium as a function of oxygen fugacity, temperature, pressure and pH (after Shock and Helgeson, 1988; Shock et al., 1989; Tanger and Helgeson, 1988).

the ore-forming pressures were within the range $(20\text{--}200)\times 10^5$ Pa; $\text{pH}=1.0\text{--}4.0$, $f_{\text{O}_2}=1.54\times 10^{-64}\text{--}1.58\times 10^{-19}$, $\text{Log } f_{\text{O}_2}=-44.55\text{--}24.62$ (Liang Xiangji et al., 1998). Variations in pressure and pH would influence the $\text{Eu}^{2+}/\text{Eu}^{3+}$ ratio slightly, but temperature and f_{O_2} could exert a strong influence, especially the latter. With increasing oxygen fugacity in the ore-forming period, the Eu anomaly would be intensified, too, thus leading to such REE distribution patterns as to be characterized by weak negative Eu anomaly, weak positive Eu anomaly and positive Eu anomaly.

It is infrequent in sulfate deposits that most ores show positive Ce anomalies. In the case of high oxygen fugacity, the ion Ce^{3+} is oxidized to the ion Ce^{4+} . The solubility of Ce^{4+} is very low, thus easy to absorb on minerals resultant from ore-forming fluids, then is concentrated in solid phase. So the alunite ores commonly show positive Ce anomalies. And the ore-forming system had abundant SO_4^{2-} , and Ce could react with SO_4^{2-} to form stable complex anions such as CeSO_4^{2+} , $\text{Ce}(\text{SO}_4)_2$, $\text{Ce}(\text{SO}_4)_3^{2-}$ and $\text{Ce}(\text{SO}_4)_4^{4-}$. At the same time, the high contents of K^+ and Na^+ in the country rocks and ores might lead to the formation of these complex salts: $\text{M}_4[\text{Ce}(\text{SO}_4)_4]\cdot n\text{H}_2\text{O}$, $\text{M}_6[\text{Ce}(\text{SO}_4)_5]\cdot n\text{H}_2\text{O}$ (Wang Zhonggang et al., 1989). All these complex ions and complex salts would exert a great influence on the occurrence of Ce anomalies.

6 Conclusions

(1) The ore-forming materials of the alunite deposit came predominantly from the igneous rocks. The ore deposition is intermediately followed by

strong metasomatism, thus making the REE distribution patterns of the country rocks and ores show significant differences.

(2) Eu anomalies are due to the variation of f_{O_2} during the ore-forming period and the alunite originated from alkaline feldspar. The structure and composition of the country rocks (especially the contents of alkaline feldspar) have important effects on the occurrence of Eu anomalies.

(3) The occurrence of Ce anomalies provides strong evidence suggesting that the Fanshan alunite deposit was formed in an acidic oxidation environment.

Acknowledgements The experiment was accomplished at the Institute of Geochemistry, Chinese Academy of Sciences and National Research Center of Geoanalysis. The authors wish to thank Hu Jian and Deng Yuejing for their help with sample analysis.

References

- Bau M. (1991) Rare-earth mobility during hydrothermal and metamorphic fluid-rock interaction and the significance of the oxidation state of europium [J]. *Chemical Geology*, **93**, 219–230.
- Bi Xianwu and Hu Ruizhong (1998) REE geochemistry of primitive ore fluids in Ailaoshan gold belt, Southwest China [J]. *Chinese Journal of Geochemistry*, **17**, 91–96.
- Boynton W.V. (1984) Cosmochemistry of the rare-earth elements meteorite studies [J]. *Geochem.*, **2**, 63–114.
- Cunningham C.G., Rye R.O., Rockwell B.W. and Kunk M.J. (2004) Supergene destruction of a hydrothermal replacement alunite deposit at Big Rock Candy Mountain, Utah: Mineralogy, spectroscopic remote sensing, stable-isotope, and argon-age evidences [J]. *Chemical Geology*, **215**, 317–333.
- Ding Zhengju, Yao Shuzhen, Liu Congqiang, Zhou Zonggui and Yang Mingguo (2003) The characteristics of exhalation-sedimentary deposit of Donggouba polymetal deposit: Evidence from ore's REE composition [J]. *Acta Petrologica Sinica*, **19**, 792–798 (in Chinese with English abstract).
- Gu Mingguang (2003) Geochemical study on volcanic rocks of the Moshishan Group in Yantou region of southeast Zhejiang [J]. *Geology and Mineral Resources of South China*, **4**, 24–30 (in Chinese with English abstract).
- Guan Tao, Huang Zhilong, Xu Cheng, Zhang Zhenliang, Yan Zaifei and Shen Baojian (2005) REE geochemistry of lamprophyres in Baimazhai nickel deposit, Yunnan Province, China: Implication for the mantle source region [J]. *Chinese Journal of Geochemistry*, **24**, 273–279.
- Hu Huaguang, Hu Shiling and Wang Songshan (1984) Isotope ages of Mesozoic-Cenozoic volcanic rocks in eastern China and adjacent area. In *Mesozoic-Cenozoic Volcanic Rocks in Eastern China and Adjacent Area* (ed. Wu Liren) [M], pp. 56. Science Press, Beijing (in Chinese).
- Hemley J.J., Hostetler P.B. and Gude A.J. (1969) Some stability relations of alunite [J]. *Economic Geology*, **64**, 599–611.
- Klinkhammer G.P., Elderfield H., Edmond J.M. and Mitra A. (1994) Geochemical implications of rare-earth element patterns in

- hydrothermal fluids from mid-ocean ridges [J]. *Geochim. Cosmochim. Acta*. **58**, 5105–5113.
- Liang Xiangji and Wang Fusheng (1998) Experimental study on formation mechanism of Fanshan alunite deposit in Pingyang, Zhejiang [J]. *Acta Geologica Sinica*. **72**, 162–172 (in Chinese with English abstract).
- Liang Xiangji, Liao Zhijie and Lan Xiang (1998) A study on some thermodynamic condition of formation of the alunite deposit in Pingsang Fanshan, Zhejiang [J]. *Geology of Zhejiang*. **14**, 35–48 (in Chinese with English abstract).
- Muthu H. Sariiz K. and Kadir S. (2005) Geochemistry and origin of the Saphane alunite deposit, Western Anatolia, Turkey [J]. *Ore Geology Reviews*. **26**, 39–50.
- Qi Liang, Hu Jing. and Gregoire D.C. (2000), Determination of trace elements in granites by inductively coupled plasma mass spectrometry [J]. *Talanta*. **51**, 507–513.
- Ren Shengli and Zhou Xinhua (1997) Geochemical and isotope chronological studies on volcanic type of super-large nonmetal deposits, Eastern Zhejiang Province [J]. *Bulletin of Mineralogy, Petrology and Geochemistry*. **16**, 7–10 (in Chinese with English abstract).
- Ren Shengli, Zhou Xinhua, Dai Tongmo and Chu Zhuying (1998) Laser micro-area analysis of ^{40}Ar - ^{39}Ar isochron age for Fanshan superlarge alunite deposit, Zhejiang Province, China [J]. *Chinese Science Bulletin*. **43**, 2005–2008.
- Shock E.L. and Helgeson H.C. (1988) Calculation of the thermodynamic and transport properties of aqueous species at high pressures and temperatures: Correlation algorithms for ionic species and equation of state predictions to 5 Kb and 1000°C [J]. *Geochim.Cosmochim.Acta*. **52**, 2009–2036.
- Shock E.L., Helgeson H.C. and Svergensky D.A. (1989) Calculation of the thermodynamic and transport properties of aqueous species at high pressures and temperatures: Standard partial molal properties of inorganic neutrall species [J]. *Geochim.Cosmochim.Acta*. **53**, 2157–2183.
- Stoffregen R.E. and Cygan G.L. (1990) An experimental study of Na-K exchange between alunite sulfate solutions [J]. *American Mineralogist*. **75**, 209–220.
- Tang Yuanlong (1992) Study of the cause of formation about the broken crater and the alunite deposit in Cangnan Fanshan, Zhejiang provinc [J]. *Geology of Chemistry*. **3**, 6–8 (in Chinese).
- Tanger I.J.C. and Helgeson H.C. (1988) Calculation of the thermodynamic and transport properties of aqueous species at high pressures and temperatures: Revised equations of state for the standard partial molal properties of ions and electrolytes [J]. *American J.Sci*. **288**, 19–98.
- Wang Fusheng, Lan Xiang and Liang Xianji (1997) The petrological characteristics and the superficial view on the cause of formation of the alunite deposit in Pingyang Fanshan [J]. *Geology of Zhejiang*. **1**, 55–63 (in Chinese with English abstract).
- Wang Zhonggang, Yu Xueyuan and Zhao Zhenhua (1989) *Geochemistry of Rare-Earth Element* [M]. pp. 15–93. Science Press, Beijing (in Chinese).
- Xie Jiaying and Tao Kuiyuan (1996) *Mesozoic Volcanic Geology and Volcano-intrusive Complexes of Southeast China Continent* [M]. pp. 98–125. Geological Publishing House, Beijing (in Chinese).
- Xuan Ziqiang (1998) Resources and tapping of alunite in China [J]. *Geology of Chemical Minerals*. **20**, 279–286 (in Chinese with English abstract).
- Yang Xiaochun (1998) REE geochemistry of the Moshishan group volcanic rocks in Yunhe-Jingning areas, Zhejiang [J]. *Journal of Chengdu University of Technology*. **25**, 254–260 (in Chinese with English abstract).
- Yang Yaomin, Tu Guamgzi and Hu Ruizhong (2004) REE and Trace Element Geochemistry of Yinachang Fe-Cu-REE Deposit, Yunnan Province, China [J]. *Chinese Journal of Geochemistry*. **23**, 265–274.
- Ye Liangfu (1931) The alunite in Pingyang, Zhejiang Province [J]. *The Publication of the Institute of Geology, Academy Sinica*. **10** (in Chinese).
- Zhou Xinhua, Ren Shengli, Chu Zhuyin and Zhang Guohui (1998) The geochemical character and isotope chronology of large, super-large typical nonmetal deposits in the east of Zhejiang Province [J]. *Science in China (Series D)*. **28**, 15–23 (in Chinese).